DETECT97 Simulation Studies of Light Output in a Full Field-of-View Small Gamma Camera

[1]M. Spisar, [1,2]J.N. Aarsvold, [3]R.A. Mintzer
[1]Department of Biomedical Engineering, [2]Department of Mathematics
University of Michigan, Ann Arbor, MI 48105
[3]Franklin McLean Memorial Research Institute, University of Chicago, Chicago, IL 60637

Abstract

Motivated by the objective of designing a full field-of-view (FOV) small gamma camera for medical applications, we investigated the limit on spatial resolution imposed by the gamma radiation detection components of three variations of one such device. For our investigation, we used a parallelized version of DETECT97 [1,2], a Monte Carlo optical photon tracking simulator. The basic component of the device simulated was an assembly comprising a 100mm x 100mm x 8mm NaI(Tl) scintillation crystal coupled to a block of quartz. We generated the point spread functions of three different crystal/quartz assemblies. The physical parameters that differed among the three assemblies were the quartz thickness and the crystal/quartz surface reflection coefficient. We performed simulations with scintillation photon generation initiated at various lateral positions within the crystal of each assembly. We emphasized positions at the periphery of the FOV of each assembly. To determine the best spatial resolution achievable by an unbiased estimator, we computed the Cramer-Rao lower bound on the variance of the position estimate for the simulated models and positions. Our computations indicate that at the centre of the FOV of each assembly the lower bound on spatial resolution is less than a millimeter and that the lower bound on resolution is less than 4mm to within 7mm of a corner of a crystal if light reflection from the side of the crystal is minimal. If light reflection from the side of a crystal is substantial, the lower bound on resolution is similar to the above in the centre of the crystal but degrades substantially 10mm from a corner of the crystal. Our computations also indicate that the estimation error correlation coefficients are generally high (|corr|~1) for peripheral source positions.

I. INTRODUCTION

The two key properties of full field-of-view (FOV) small gamma cameras are: 1) minimal housing to allow the active area to be positioned as close as possible to a source distribution; and 2) an active detector area identical in size to the area enclosed by the camera housing. The first property is a characteristic of several cameras that have been developed; the second a characteristic of few. The objective of our study is an improved understanding of the limits on spatial resolution imposed by the gamma radiation detection components of full FOV devices utilizing single NaI(Tl) scintillation crystals coupled to quartz. The simulations conducted did not model a photodetector or an array of photodetectors.

An example of a full FOV small gamma camera is a University of Arizona (UA) modular detector [3,4]; it has four photomultiplier tubes (PMTs). A UA module's single scintillation crystal and active detection area are both 10cm x 10cm; a UA module's housing and shielding are less than 1 cm thick when it is configured as a simple imager. An example of a camera that does not have a full FOV is the University of Chicago (UC) small gamma camera, which utilizes a single position-sensitive photomultiplier tube (PSPMT) [5,6]. The UC camera's single scintillation crystal is 7.6cm x 7.6cm, while its active detection area is 6.5cm x 6.5cm; its housing and shielding are less than 1cm thick. Our interest is the class of detectors that includes the UA module.

For small full FOV cameras, the peripheral regions of the FOV are the crucial regions in which spatial resolution must not deteriorate to any great extent. We carried out simulations to isolate the influence of the scintillator and quartz assembly on the point spread function (PSF). The effect on spatial resolution (as a function of source position) was quantified by computing the Cramer-Rao lower bound (CRLB) on variance of the position estimate for each model and source position simulated; we simulated a greater number of peripheral sources than centrally located sources.

The parameter estimates may be expressed as a function of the probability distribution (pdf) of the measurements conditioned by the parameters. The Cramer-Rao lower bound is an application of the Schwartz inequality to the covariance matrix of the parameter estimates expressed in this manner. The set of parameters one generally seeks to estimate in gamma-ray imaging includes the x, y, and z coordinates of a scintillation event and the energy of the incident gamma ray. In this study, we fixed the gamma-ray energy to be 140keV. This energy corresponds to the energy of technetium-99m, an isotope frequently used for medical imaging. We also fixed z in each simulation. Thus, in this study, x and y were the only parameters to be estimated. Let $\theta = [\theta_x, \theta_y] = [x,y]$ represent this set of parameters.

0-7803-4258-5/98/$10.00 © 1998 IEEE

In our study, each crystal/quartz assembly had an exit surface with dimensions 100mm x 100mm. In the simulations, we binned the optical photons exiting this surface into the pixels of a 64x64 grid. The 64x64 pixel mapping of the light distribution generated in each simulation provided a set of values dependent on the parameters to be estimated; let the values (the data, the measurements) be represented by $m=[m_1,...,m_{4096}]^t$. If we assume that the emission of a gamma ray is a Poisson-distributed event and that the number of scintillation photons produced at an interaction site in a crystal is a deterministic number, it follows that the m_i are Poisson-distributed. The latter assumption is, in fact, a condition not valid in reality; the number of scintillation photons produced by a 140keV gamma ray in NaI(Tl) has a mean of about 5,200, but this number is not noise-free. However, the Poisson assumption is reasonable, and we use it to simplify the analysis.

Assume the conditional pdf, f(m|θ), is Poisson. Given an estimator $\Theta = \Theta(m)$, its covariance is given by:

$$K_\Theta = E[(\Theta(m) - E(\Theta(m)))(\Theta(m) - E(\Theta(m)))^t] ,$$

where *E[•]* is expectation. Application of the Schwartz inequality to the above yields the Cramer-Rao lower bound on the covariance matrix of the estimator:

$$(1) \qquad K_\Theta \geq [E[\nabla_\theta{}^2 \ln f(m \mid \theta)]]^{-1} .$$

Our assumption that f(m|θ) is Poisson leads to the conclusion that:

$$(2) \qquad K_\Theta - [(\nabla_\theta m(\theta))^t (diag(m(\theta))^{-1} (\nabla(m(\theta))]^{-1}$$

is a non-negative, definite matrix.

Accordingly, the diagonal elements of the second matrix of (2) are interpreted as the lower bounds on the variances and covariances of the parameters with which they are associated. Because the parameters are the x and y coordinates of the source location, there is an immediate correspondence with the spatial resolution of the crystal/quartz assembly being considered.

The Cramer-Rao approach to establishing a lower limit on spatial resolution for modular detectors has been utilized by Clinthorne et al. [7]. Milster [3] has used the technique in the analysis of position estimation in the UA modular detectors. Strobel [8] has used it to establish the degree of improvement in resolution achievable with corner cubes added to the entrance face of a CsI(Tl) scintillator.

Spatial resolution is influenced by the number and location of detectors. Spatial resolution is also dependent on the geometries of, and optical finishes applied to, the scintillation crystal and glass support of the detector. Subtleties such as crystal grind finishes, which may vary with manufacturer, are beyond the scope of this study — we wish only to establish a quantification of the spatial resolution limit imposed by parameters that can be easily specified in the construction of the crystal/quartz assembly of a small gamma camera. We simulated the effects of varying two parameters: the quartz (support) thickness and the side reflection coefficient of the crystal and quartz.

II. Methods

DETECT97 [1,2] — a Monte Carlo optical photon tracking simulator — was used to generate the point spread functions of three different crystal/quartz assemblies. In order to facilitate the running of a statistically sufficient number of photon simulations, we implemented a parallel version of DETECT97. In the parallel implementation each simulation is independent of the others; parallelization reduced the execution time for multiple simulations by a factor equal to the number of processors utilized. We also replaced the random number generator in DETECT97, because correlations on a small scale had been found in the testing of the original random number generator [9].

The basic configuration of the three models simulated is illustrated in Figure 1. The lateral dimensions ('x' and 'y') of the simulated crystal were 100mm x 100mm. The centre of the crystal was assigned lateral coordinates (50,50), and one corner was assigned coordinates (100,100).

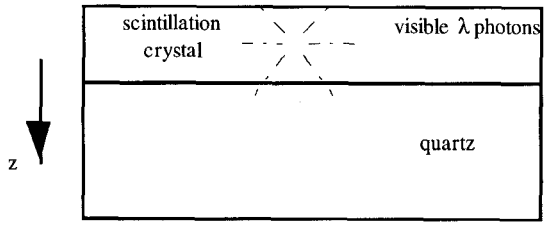

Figure 1 Schematic of basic crystal/quartz configuration

Together with specification of the number and the originating position of scintillation photons, the simulated models served as the input to our parallelized version of DETECT97. The output file of each simulation was a 64x64 matrix representing the light distribution at the exit surface of the quartz support.

For each source position investigated, simulations were also conducted with the source displaced by 1mm in the x and, independently, 1mm in the y directions. This enabled us to establish a finite gradient associated with the particular source location. We used the three sets of data to compute the Cramer-Rao lower bound and thus obtained the correlation coefficient for x and y estimation errors, as well as the lower limit on spatial resolution achievable by an unbiased estimator.

The base model used for the crystal/quartz assembly had a crystal thickness of 8mm and a quartz support thickness of 15mm. The sides (parallel to 'z') of the crystal/quartz assembly were assigned a reflection coefficient of 5%, while

the entrance face of the crystal was assigned a reflection coefficient of 98%. The two variations on the base model included one with a higher reflection coefficient (50%) on the sides (potentially effected by applying a reflecting coating, as opposed to a matte finish) and one with a thinner quartz support (5mm). Table 1 summarizes the key model parameters and their variations.

PARAMETER ↓	MODEL →	BASE	RC=50% ON SIDES	5MM QUARTZ
crystal entrance face reflection coefficient		98%	98%	98%
crystal thickness		8mm	8mm	8mm
quartz thickness		15mm	15mm	**5mm**
side paint reflection coefficient		5%	**50%**	5%

Table 1 : Simulation model names and parameters

In order to determine parameters of particular utility to a full FOV camera, the source positions that we simulated were: the centre of the crystal, a point midway between the centre and the (100,100) corner (along the diagonal), and several points near the corner (also along the diagonal).

The simulation code itself imposes limits on the physical accuracy of the models. In the interest of decreasing the time required per simulation, we used the simplified model just described. Normally, the crystal and quartz are joined by a layer of optical coupling compound, as are the quartz and photodetector(s) of a small camera of the type modeled. We conducted a short series of simulations using a model that included coupling compound between the crystal and quartz and between the quartz and a photodetector. The results of those simulations were only marginally different from those of the simplified model. Thus, in the interest of reducing computation time, we omitted those layers from our simulated models reported here.

We used MATLAB to process the binary, 64x64 pixel point spread functions, and to carry out all Cramer-Rao lower bound computations.

III. RESULTS

A grouping of the 64x64 pixel image into an NxN matrix represents the effect of employing N^2 ideal detector elements. The effects of detector number and model parameters are inextricably interrelated, and we analyzed the data in two ways. Initially, we considered all three sets of model parameters, coupled with a fixed number of detectors. Results are displayed in Figure 2 for 32x32, 4x4, and, 2x2 detector elements.

Next, we determined the CRLB on spatial resolution as a function of the number of detector elements, keeping the model parameters constant. Graphs showing the results of this analysis are given in Figure 3.

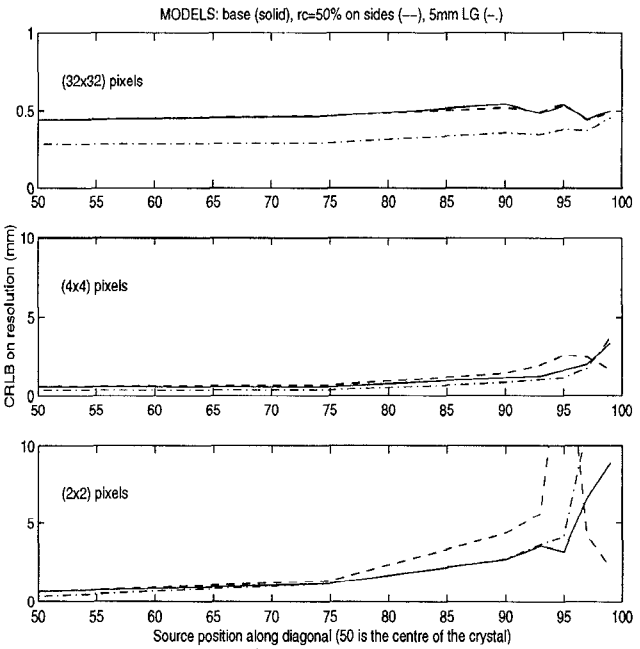

Figure 2. CRLB vs. source position for simulated models

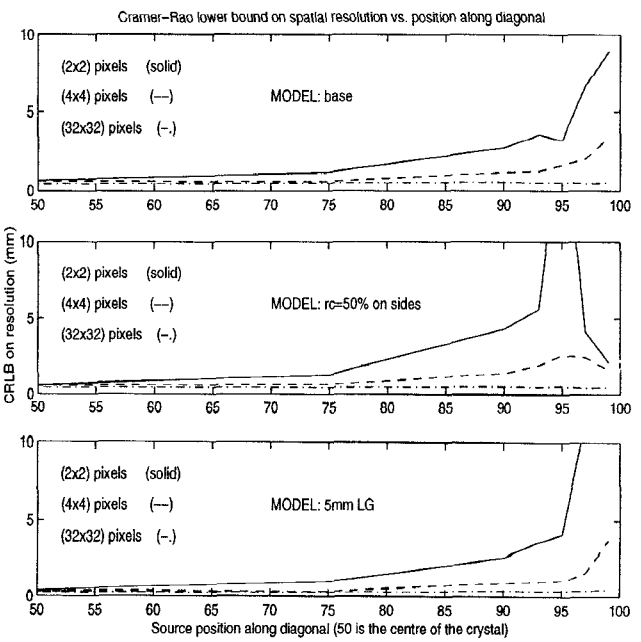

Figure 3. CRLB vs. source position as a function of number of detectors

The depth of interaction (DOI) in the crystal is normally not a known quantity in currently available small gamma cameras. Due to the increased interest in effects due to the variation in depth of interaction, we present estimates for the limiting spatial resolution for interactions occurring at depths of 1mm and 4mm into the 8mm thick crystal (Figure 4).

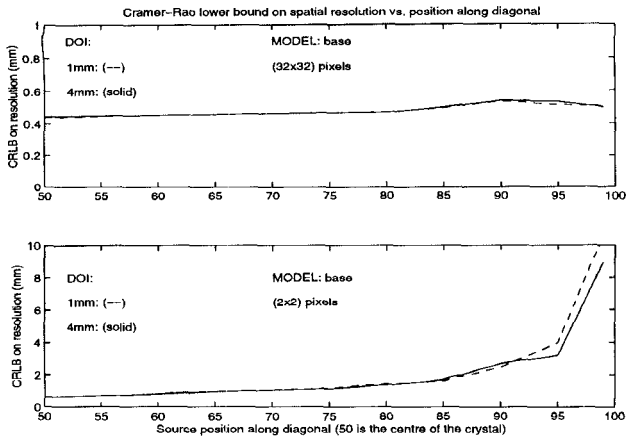

Figure 4. CRLB vs. source position for different (fixed) DOIs

Finally, examples of spatial variation of the coefficient of correlation (between position estimation errors in x and y) are produced in Figure 5.

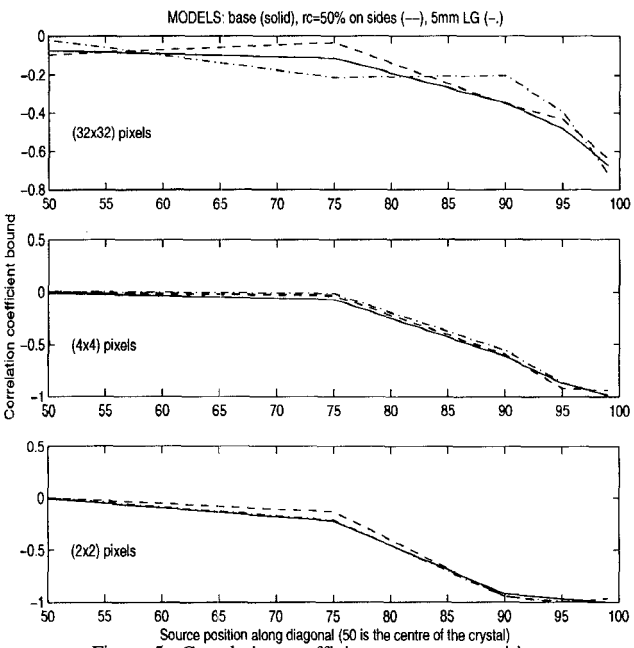

Figure 5. Correlation coefficient vs. source position

IV. Discussion

Using 32x32 detector elements, and making comparison with the base model, the relative effect on spatial resolution produced by an increase of the side reflection coefficient (from 5% to 50%) was negligible (Figure 1). For fewer (4x4 and 2x2) detector elements, degradation of the limiting resolution between diagonal positions 75 and 95 was evidenced, but the limit on resolution was enhanced at the very corner (>95). Because the lower bound depends on the gradient of the PSF, this is not a surprising result. As the source approaches the side of the crystal, a greater solid angle subtended by direct scintillation photons is intercepted by the crystal wall. The high reflection coefficient causes a larger percentage of the photons to be reflected to the other side of the crystal, and the gradient on which the bound depends is enhanced.

The model with the reduced quartz thickness (5mm, rather than 15mm), exhibited behaviour similar to that of the base model, with a somewhat enhanced resolution limit between the centre and position 95 for 4x4 and 2x2 pixels (Figure 1). At some point between 95 and 99, the trend reversed, and the resolution limit of this model deteriorated rapidly. This phenomenon is attributed to the decreased gradient associated with fewer light photons reaching the detectors at the distant lateral corner from the source x-y location.

Examination of the Cramer-Rao lower bound and its variation with number of detector elements reveals a dependence on source position (Figure 2). For the three models, the improvement in resolution from 2x2 detector elements to 4x4 detector elements was at least twofold at almost all source locations. As expected, the resolution with 32x32 detector elements was superior in all cases. Results regarding the variation (by 3mm) in depth of interaction (Figure 3) were almost identical in the centre of the FOV, and varied little at the corner.

It has been noted [3,10] that the image of a pseudo-point source near the corner of the FOV experiences a 'warping' effect. The correlation coefficient results (Figure 5) are consistent with these observations, in that the absolute values approach 1 (maximum) near the corner, while remaining depressed elsewhere. The interpretation of this correlation coefficient is that the degree of error in the estimate of one of the position parameters is strongly related to the degree of error in the estimate of the remaining position parameter. These high correlations lead to ellipses on which the position estimates for a pseudo-point source reside.

V. Conclusions

We have investigated the limit on spatial resolution imposed by the crystal and quartz components of a small gamma camera. A parallelized version of DETECT97 was used to generate the point spread functions of three different scintillation crystal and quartz assemblies. With respect to a base model, one model had a thinner block of quartz, while the other had a significantly more reflective side finish. Cramer-Rao lower bound calculations indicated that resolution near the centre of the FOV was limited to less than a millimeter for all sets of parameters. Both the base model and the model with thinner quartz maintained limits of less than 4mm resolution to within 7mm of the edge of the crystal. The CRLB corresponding to the model with higher reflection coefficient underwent a sharp increase as the source approached the corner, but that trend reversed and associated very low bounds on resolution with sources that were extremely close to the corner. We found that the estimation error correlation coefficients were generally high (|corr|~1) for peripheral source positions.

VI. Acknowledgements

This work was sponsored by NIH grant #5R29NS35765-02, a University of Michigan Rackham Grant, and the University of Michigan Biomedical Engineering Program.

The authors thank W.L. Rogers and N.H. Clinthorne, University of Michigan, for many invaluable discussions regarding this work. They also thank C. Moisan, et al, TRIUMF, for the translation of DETECT to DETECT97, and H. Marshall, University of Michigan Center for Parallel Computing (partially funded by NSF grant CDA-92-14296) for assistance in parallelizing DETECT97.

VI. References

[1] A. Levin, E. Hoskinson, and C. Moison. DETECT97: A program for modeling optical properties of scintillators, 1996.

[2] G.F. Knoll and T.F. Knoll. DETECT: A program for modeling optical properties of scintillators, 1988.

[3] T.D. Milster. Design and construction of a modular gamma camera. Ph.D. Dissertation, University of Arizona, 1987.

[4] T.D. Milster, J.N. Aarsvold, H.H. Barrett, A.L. Landesman, L.S. Mar, D.D. Patton, T.J. Roney, R.K. Rowe, and R.H. Seacat III. A full-field modular gamma camera, *J. Nucl. Med.*, 31(5):632-639, 1990.

[5] N.J. Yasillo, R.A. Mintzer, J.N. Aarsvold, R.N. Beck, T.A. Block, C.T. Chen, M. Cooper, S.J. Heimsath, K.L. Matthews II, C.E. Ordonez, X. Pan, and C. Wu. A single tube gamma camera for clinical imaging, *Conf. Rec. of the 1993 IEEE NSS/MIC*, vol. 2, 1073-1076, 1994.

[6] J.N. Aarsvold, R.A. Mintzer, N.J. Yasillo, S.J. Heimsath, R.N. Beck, C.-T. Chen, M. Cooper, T.A. Block, K.L. Matthews II, X. Pan, and C. Wu. A miniature gamma camera, in *Electrical Injury: A Multidisciplinary Approach to Therapy, Prevention, and Rehabilitation* (R.C. Lee, M. Capelli-Schellpfeffer, and K.M. Kelly; eds). Annals of the New York Academy of Sciences, vol 720, 192-205, 1994.

[7] N.H. Clinthorne, W.L. Rogers, L. Shao, and K.F. Koral. A hybrid maximum likelihood position computer for scintillation cameras, *IEEE Trans. Nucl. Sci.*, 34(1):97-101, 1987.

[8] J. Strobel. Design and evaluation of the scintillator surface on CsI(Tl) for a high resolution solid state gamma camera. (thesis) Technische Universitat Munchen, 1996.

[9] Scott Wilderman, Department of Nuclear Engineering and Radiological Sciences, University of Michigan, personal communication, 1997.

[10] Aarsvold JN, Mintzer RA, Matthews KL II, Yasillo NJ, Ordonez CE, Chen C-T, and Beck RN. Implementations of maximum-likelihood position estimation in a four-PMT scintillation detector. *Conference Record of the 1995 IEEE NSS/MIC*, 3:1811-1815, 1996.